RESEARCH ARTICLE | SEPTEMBER 24 2015

Internal quantum efficiency enhancement of GaInN/GaN quantum-well structures using Ag nanoparticles

Daisuke Iida; Ahmed Fadil; Yuntian Chen; Yiyu Ou; Oleksii Kopylov; Motoaki Iwaya; Tetsuya Takeuchi; Satoshi Kamiyama; Isamu Akasaki; Haiyan Ou

AIP Advances 5, 097169 (2015)
https://doi.org/10.1063/1.4931948

Internal quantum efficiency enhancement of GaInN/GaN quantum-well structures using Ag nanoparticles

Daisuke Iida,[1,2,3] Ahmed Fadil,[2,a] Yuntian Chen,[2,4,b] Yiyu Ou,[2] Oleksii Kopylov,[2] Motoaki Iwaya,[3] Tetsuya Takeuchi,[3] Satoshi Kamiyama,[3] Isamu Akasaki,[3,5] and Haiyan Ou[2]

[1]*Department of Applied Physics, Tokyo University of Science, Katsushika, 125-8585 Tokyo, Japan*
[2]*Department of Photonics Engineering, Technical University of Denmark, 2800 Lyngby, Denmark*
[3]*Faculty of Science and Technology, Meijo University, 1-501 Shiogamaguchi Tempaku, 468-8502 Nagoya, Japan*
[4]*School of Optical and Electronic Information, Huazhong University of Science and Technology, 430074 Wuhan, China*
[5]*Akasaki Research Center, Nagoya University, Furo-cho Chikusa, 464-8603 Nagoya, Japan*

(Received 22 May 2015; accepted 16 September 2015; published online 24 September 2015)

We report internal quantum efficiency enhancement of thin p-GaN green quantum-well structure using self-assembled Ag nanoparticles. Temperature dependent photoluminescence measurements are conducted to determine the internal quantum efficiency. The impact of excitation power density on the enhancement factor is investigated. We obtain an internal quantum efficiency enhancement by a factor of 2.3 at 756 W/cm^2, and a factor of 8.1 at 1 W/cm^2. A Purcell enhancement up to a factor of 26 is estimated by fitting the experimental results to a theoretical model for the efficiency enhancement factor. [http://dx.doi.org/10.1063/1.4931948]

I. INTRODUCTION

An efficient high-brightness solid-state lighting solution is of central industrial and social relevance in terms of reducing energy consumption and environmental benefits. The GaInN-material based light-emitting diodes (LEDs) technology appears to be an excellent candidate in solid-state lighting platform. Improving the LEDs performance within the green gap is challenging, and is also a major focus in the research efforts of GaInN-based LEDs. The LEDs grown on c-plane sapphire substrate have a large piezoelectric field in the quantum well (QW) due to quantum confined Stark effect (QCSE).[1,2] The large piezoelectric field is one of the most critical factors limiting the internal quantum efficiency (IQE) in the green gap. In order to improve GaInN-based LEDs both enhancement of the IQE and development of an efficient light extraction techniques to 'drag' the photons out of the LED crystal are required.[3,4] It is well known that spontaneous emission, including the recombination rate and the emission profile, can be modified by the nearby photonic environments.[5,6] The key concept underlying plasmon enhanced light emission is the local density of optical states (LDOS), which accounts for the available number of modes per frequency at a certain position. Recent progress in nanophotonics and nanotechnology opens possibilities of engineering LDOS at nanometer scale and at highly advanced levels to achieve directional emission or enhanced light-matter interaction.[7–14] Such a nanophotonic approach has been applied to light emitting devices.[15–22,24,25] The rationale behind is that the transfer of energy from carriers in GaInN QW into localized optical plasmon supported by the metallic nanostructures will create an

[a]afad@fotonik.dtu.dk
[b]yuntian@hust.edu.cn

additional light emission channel called plasmonic channel. With a thin p-GaN layer plasmonic channel will dominate the spontaneous emission and significantly enhance the radiative recombination rate of light sources. As the rate of emitted photons is enhanced compared to the undesired non-radiative channels, which are unaffected by the plasmonic structures, we expect to overcome the challenge on IQE. Subsequently, the radiation captured by the plasmonic structure needs to be scattered into desired output angles by designed grating effects from periodic plasmonic structures or by exploiting random scattering from disordered plasmonic structures. Indeed, the IQE measurement of blue emission GaInN QWs indicates that significant plasmonic coupling can be achieved at approximately 6.8-folds when the distance of the active layer to the metals (D) is very small, i.e. ~10 nm.[3] The blue LEDs having a small D of 30 nm is reported to have enhanced optical output power by 38% using the nanoparticles embedded in p-GaN.[17] For a larger D of approximately 70 nm, the green emission output power based on the plasmonic coupling of the metals with active layer has been improved by approximately 90-220% with contribution from both IQE and light extraction efficiency.[16] It is also very interesting to note that the photoluminescence (PL) intensity of the green GaInN QW has been improved by a factor of 4.8 using periodic nanocylinders with a 5 nm spacing layer.[20] It has been shown that for very large D ~200 nm, a 26% improvement of the optical output power due to enhanced light scattering can be achieved without benefits from plasmon enhanced IQE.[19] Despite the aforementioned evidences on improved PL or electroluminescence (EL) emission, to the best of our knowledge, there is no quantitative study of how original emitter IQE affects the enhancement obtainable through LSP-coupling between metal and emitter.

In this paper, we experimentally demonstrated the IQE enhancement of plasmon-based LED epi-structures by depositing metallic nanoparticles on top of the GaN crystal using a low-cost solution. The IQE is estimated from low temperature PL measurements. We perform excitation power density dependent measurements, which show the IQE can be substantially enhanced with properly selected nanometallic structure. The paper is organized as follows: In section II, we outline the fabrication procedures of our LED structures and the metallic nanoparticles, and demonstrate the measurement setup. In section III, we present and discuss our experimental results of PL and IQE enhancement. Finally, section IV concludes the paper.

II. METHODS

LED structures were grown by metalorganic vapor phase epitaxy (MOVPE) in a horizontal flow reactor. C-plane sapphire substrates were thermally cleaned in a H_2 ambient at approximately 1050 ºC. After that, approximately 20-nm-thick low temperature (LT)-GaN buffer layer was deposited at 535 ºC.[23] After annealing process a 2-μm-thick GaN layer was grown at 1050 ºC on the annealed LT-GaN nucleation layer. The final LED structure consisted of a 2-μm-thick n-GaN:Si layer, a 10 periods of GaInN:Si (3 nm) / GaN:Si (2 nm) superlattice layer, a 5 periods of GaN:Si (11.5 nm) / GaInN (2 nm) QWs active region covered with 5-nm-thick GaN capping layer, a 20-nm-thick p-GaN:Mg, and a 5-nm-thick p^+-GaN:Mg p-contact layer. The distance of last QW to LED surface was 30 nm. This LED structure had an optimized thin p-GaN layer for coupling of localized surface plasmon (LSP) to QWs, which is expected to enhance the light emission of QWs with LSP coupling. Self-assembled Ag NPs were fabricated by electron-beam evaporation and thermal annealing. Various-thickness Ag thin films were deposited on top of the LED surface. The samples were annealed at 200 ºC for 30 min in N_2 atmosphere. Ag thin film was transformed into random nanostructures during thermal annealing process.

The observations of Ag NPs on top of the LED surfaces were conducted by scanning electron microscope (SEM). Excitation power density dependent PL measurement was carried out to characterize the emission of GaInN/GaN QWs grown on c-plane sapphire substrate. The PL measurement setup consisted of a continuous wave GaInN-based diode laser and a spectrometer. The excitation laser operated at 405 nm and the output power density could be tuned from 1 to 756 W/cm^2. PL measurement was carried out with excitation and collection via the backside of the polished sapphire substrate. The extinction spectrum of Ag NPs was extracted from a transmittance spectrum measurement. Transmittance was measured from the sapphire to the top surface p-GaN side, while

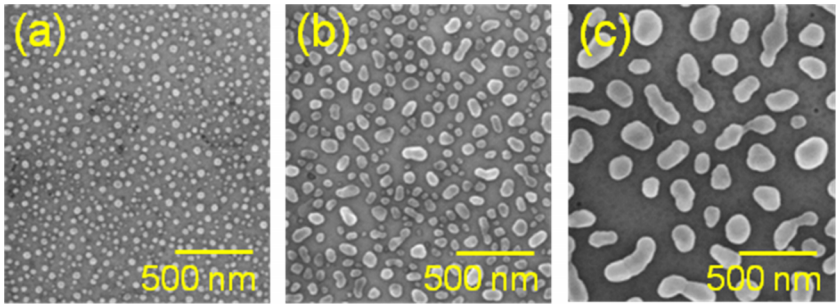

FIG. 1. SEM images of Ag NPs on LED surface after thermal annealing process. Ag deposition thicknesses are (a) 4 nm (sample A), (b) 9.5 nm (sample B) and (c) 17 nm (sample C), respectively.

reflectance was measured from the sapphire side. The light source used for the measurements was a white-light Xenon lamp.

III. RESULTS AND DISCUSSIONS

A. Self-assembled Ag NPs

The Ag NPs were fabricated using a low-cost approach, i.e. by thermal annealing of Ag thin films on the surface of LED structure with designed thin p-GaN layers. Fig. 1 shows plan-view SEM images of Ag NPs with different Ag deposition thickness. Samples A, B and C are Ag films with a thickness of 4, 9.5 and 17nm, respectively, which are transformed into random NPs after thermal annealing on top of the LED p-GaN surface. As the Ag film thickness increases, the size of Ag NPs becomes larger, while the density of Ag NPs decreases. Ag NPs had a tendency of becoming more irregular-shaped and with an increased size distribution as the thickness was increased.

Fig. 2 shows the extinction spectra of the three samples. PL emission spectrum of GaInN/GaN 5QWs LED without Ag NPs constituting a reference sample is also shown in Fig. 2. Considering the extinction spectra, each sample shows a characteristic peak. For sample A the extinction peak is located at 482 nm, and the peak position of sample B is 540 nm, while the main peak position of sample C is 672 nm. In the case of sample C a smaller peak is visible in the extinction spectrum at 410 nm. We attribute these peaks to the dipolar resonances in the NPs, hence for sample C a higher order mode is present at short wavelengths.[20] It is seen that the peaks red-shift with increasing average particle size, while the full width at half maximum (FWHM) increases. These self-assembled Ag NPs have different sizes and spacing, and this will in principle give rise to an inhomogeneous broadening of the LSP resonances from the distribution of the particle sizes.

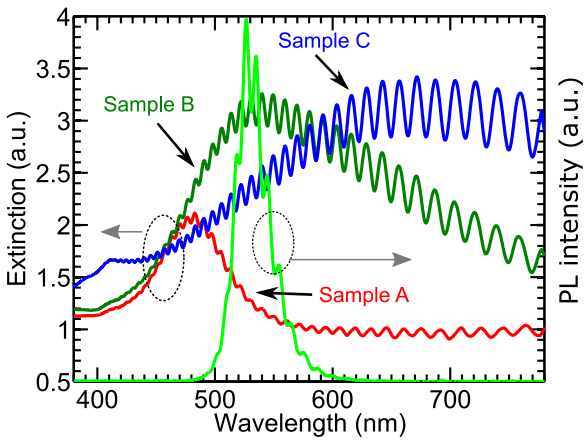

FIG. 2. Extinction spectra for samples A, B and C. Reference PL spectrum is shown for comparison.

Sample A has the most regular-shaped NPs with a small spread in size distribution, and is in effect showing a resonance peak with the smallest FWHM. Resonance peak of sample C seems to be located at around 700 nm, but has a large FWHM in contrast, the tail of which is covering the QWs emission spectrum. Sample B had a better spectral overlap with the QWs emission than the other Ag NPs structures. It is therefore expected that LSP coupling with QWs of sample B can be the most pronounced. The resonance peaks shift towards longer wavelengths as Ag NP size increases due to the red-shift of the dipolar resonance for larger diameter, as long as the dipole approximation is valid.[9]

B. PL measurements

We investigated PL enhancement of GaInN/GaN QWs with various Ag NPs. For PL measurements the sample excitation and emission collection were done from the backside of the polished sapphire substrate, and the spectra measured at room temperature are shown in Fig. 3. It is seen that the PL emission of sample A has remained nearly unchanged compared to the bare LED emission, while PL enhancements are observed for sample B and C. Increasing the Ag thickness, hence also the average particle size, results in an increase in PL enhancement. The integrated PL enhancements of samples A-C relative the reference sample are 1.25, 2.59 and 6.02, respectively.

Other mechanisms could exist behind the PL enhancement in addition to LSP-QW coupling. One is an enhanced reflection from the top p-GaN surface of either the excitation laser signal, and/or the emission from the QWs, both of which would give an enhanced signal at the detector. The reflectance spectra (not shown) reveal that the Ag NPs formed on the p-GaN surface do not result in an increased reflection compared to the as-grown surface at the QWs emission wavelength. At the excitation wavelength the reflection is enhanced by 10 %, which results in an insignificant enhancement factor that is already taken into account in Fig. 3.[20] These factors are therefore excluded.

C. Temperature dependent PL

We proceed to study the improvement of the IQE based on temperature dependent PL. We analyzed the IQE of the LEDs with various Ag NPs by measuring PL intensity versus temperature, as shown in Fig. 4. Under the assumption that non-radiative recombinations are inactivated at cryogenic temperatures, one can retrieve the IQE from the temperature dependence of integrated PL intensity I.[26] The IQE is defined by normalizing the integrated PL intensity to 1 at 20 K, i.e., assuming the IQE to be 100 %. Thus, the IQE at room temperature will be defined

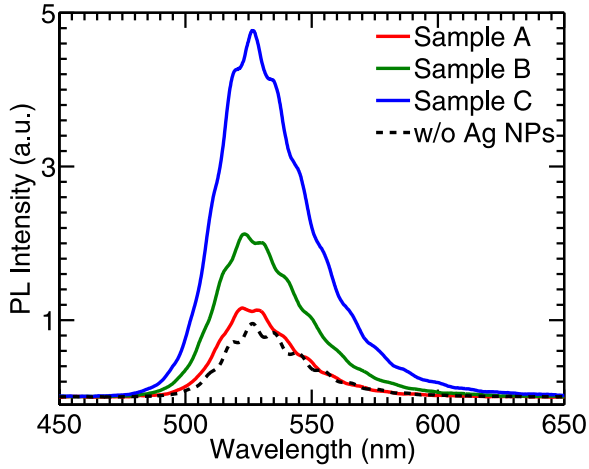

FIG. 3. Room temperature PL intensity of GaInN/GaN 5QWs with Ag NPs on top. Excitation power density is 756 W/cm^2, and emission peak is around 530 nm.

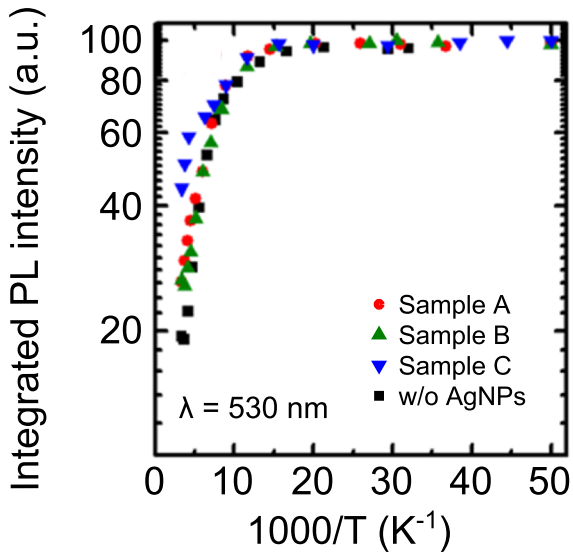

FIG. 4. Temperature dependence of integrated PL for estimating IQE. PL intensity has been normalized to 100 at the 20 K value.

as IQE = I_{295K}/I_{20K}. As the temperature increases, PL intensity degrades due to the activation of non-radiative recombination process. The IQE for the 530 nm emission was found to be 19.3 % for the reference sample. Regarding the Ag NP coated samples, the expression for the IQE will be modified due to LSP-coupling, $\eta = (k_{rad} + k_{SP}\eta_{LSP})/(k_{rad} + k_{nrad} + k_{SP})$, where k_{rad}, k_{nrad} and k_{SP} are the radiative, non-radiative and LSP coupling rates, and η_{LSP} is the radiative coupling efficiency of the LSP mode. It has been demonstrated that k_{SP} and k_{nrad} follow similar trends as a function of temperature, and it is therefore reasonable to estimate $k_{SP} \sim 0$ at low temperatures and assume that IQE is approximately 100 % for the Ag NP coated samples.[27] We can then estimate the IQE of samples A-C the same way as the reference, and obtain 26.1 %, 26.4 % and 44.2 %, for samples A, B and C, respectively, with 756 W/cm^2 of excitation power density. Table I summarizes the IQE enhancement factors.

We note that the IQE of A is almost equal to that of B, and higher than the reference sample IQE, contrary to what was observed in the PL measurements of Fig. 3 where sample B had a considerably higher PL intensity. The integrated PL intensity is proportional to the external quantum efficiency, and as such it includes the effects of both IQE and light extraction efficiency (LEE). The observed difference between the integrated PL and IQE enhancement factor suggests a modified LEE for samples A-C. The IQE enhancement of sample A is higher than its integrated PL enhancement which indicates a degraded LEE. As for samples B and C is it seen that the integrated PL intensity has a higher enhancement than the IQE. Assuming the integrated PL intensity is proportional to the external quantum efficiency (EQE), the LEE enhancement can be estimated through the ratio between integrated PL enhancement and IQE enhancement. This follows since the integrated PL enhancement can be written as $I_{Ag}/I_{ref} = LEE_{Ag}/LEE_{ref} \times IQE_{Ag}/IQE_{ref}$. The LEE

TABLE I. Summary of enhancement parameters. Also given is the LSP radiative efficiency and Purcell factor obtained from power density variation and the relation between IQE enhancement and initial IQE.

Sample	Avg. size [nm]	Integrated PL enhancement[a]	Deduced LEE enhancement	High power IQE enhancement[b]	Low power IQE enhancement[b]	η_{LSP}	F_P
A	50	1.25	0.93	1.35	1.10	-	-
B	120	2.59	1.90	1.36	1.71	0.38	2.4
C	185	6.02	2.63	2.29	8.12	0.45	26.5

[a]At 295 K, and 756 W/cm^2 excitation power.
[b]High power: 756 W/cm^2, Low power: 1 W/cm^2.

ratios for samples A-C are listed in Table I, where sample B and C show an enhancement by a factor of 1.9 and 2.6, respectively, while A shows a reduced LEE based on these estimations.

The improved LEE due to Ag NPs is observed from sapphire-side emission, and is expected to be coming from the scattering of Ag NPs acting on the QW emission, i.e. the radiatively emitted light from the QWs that are not coupled to LSP modes. The emitted light from the QWs will see a modified interface when Ag NPs are included compared to a bare GaN-air interface, and this is expected to change the LEE.[27] In the following we will direct our attention to the IQE enhancement caused by the Ag NPs.

D. Excitation power density dependent IQE

We continue to study the excitation power density dependent IQE, which further supports the conclusion of improved IQE due to plasmonic coupling from temperature dependent PL measurement. In Fig. 5(a) we obtain the IQE at various excitation power densities for the emission point with 530 nm peak wavelength at 756 W/cm^2. We first note the increasing IQE of the reference sample with increasing power densities. This effect is attributed to coulomb screening of the quantum-confined stark effect (QCSE) by the increasing carrier density.[28]

Fig. 5(b) shows the IQE enhancements with changing excitation power density. The trend for samples B and C is a decreasing enhancement with power density, while for sample A the opposite trend is observed, although weak. It is also noticed that the enhancements factors for sample A and B approach each other at high power density.

To understand the decrease in IQE enhancement, we need to keep in mind the increase in original (reference sample) IQE with increasing power density. The observed trend is that the lower the initial IQE is, the higher the enhancement factor is due to LSP coupling, and this is in agreement with the theoretical expectation of an inverse relation between IQE enhancement due to Ag NPs, K, and initial IQE without Ag NPs, η_i, which can obtained as the ratio,[29]

$$K = \frac{(k_{rad} + k_{SP}\eta_{LSP}) / (k_{rad} + k_{SP} + k_{nrad})}{k_{rad} / (k_{rad} + k_{nrad})} = \frac{1 + F_p\eta_{LSP}}{1 + F_p\eta_i}, \quad (1)$$

where $F_p = k_{SP}/k_{rad}$, is the Purcell enhancement factor, and η_{LSP} is the radiative efficiency of the LSP-mode. This relation also implies that the requirement for IQE enhancement, i.e. $K > 1$, the LSP-mode radiative efficiency has been to be larger than the initial IQE, $\eta_{LSP} > \eta_i$. We plot the IQE enhancement factors of Fig. 5(b) as a function of the initial IQE in Fig. 6. The inverse relation is most clear for sample C, while sample B shows a similar but weak trend. For sample A, the opposite trend is observed. Using Eq. (1) we can roughly fit the data in Fig. 6 to obtain both the Purcell factor and the radiative efficiency of the Ag NPs. From these measurements, we estimate a Purcell enhancement factor of 26.5 and an LSP radiative efficiency of 45 % for the Ag NPs of sample C. The values obtained for sample B are 1.7 for the Purcell and 38 % for LSP radiative

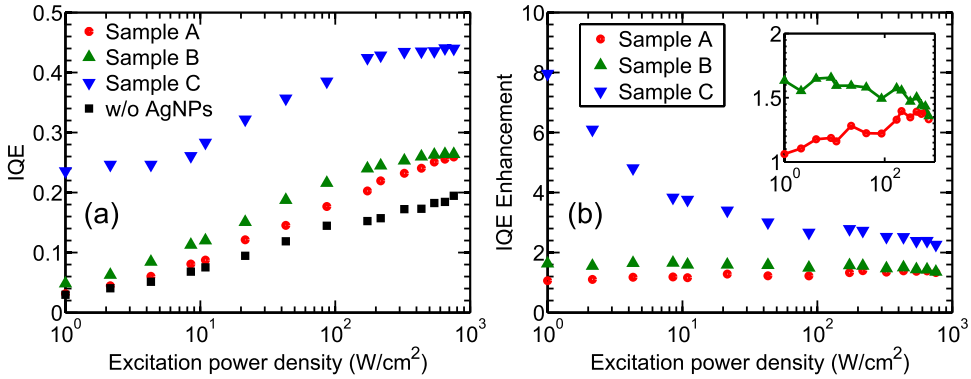

FIG. 5. (a) The estimated IQE and (b) IQE enhancement factor as a function of excitation power density at 295 K. Inset is the zoom in for sample A and B.

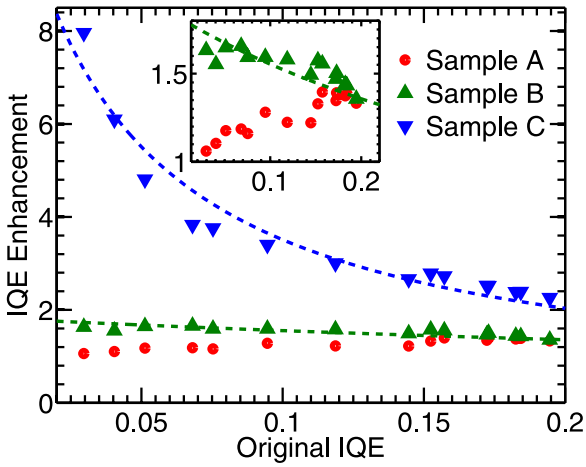

FIG. 6. IQE enhancement factor with initial IQE variation, calculated from the measurements of excitation power density variation. Dashed lines are fittings based on Eq. (1). Inset is the zoom-in at small IQE enhancement factor for sample A and B .

efficiency. The results are summarized in Table I. Due to the opposite trend observed for sample A, no parameters could be obtained. The difference in Purcell factors between sample B and C imply different LSP-QW coupling rates, where C has a higher coupling rate than B. Through numerical calculations we have previously investigated the decay rate enhancement in the plane of the QWs from Ag NPs, and have found that larger NPs exhibit larger enhancement factors for particle sizes up to about 200 nm in diameter.[30] The difference in average Ag NP size between sample B and C explains why the Purcell factor of C is larger than B.

As seen from the extinction spectra, the LSP resonance of sample A is blue-shifted relative to the emission peak, while those of B and C are red-shifted. When increasing the excitation power density, in addition to the increase in IQE, the GaInN/GaN QWs peak emission wavelength is blue-shifted due to the screening piezoelectric field by free-carriers.[31,32] For the reference sample the emission peak around 528 nm is red-shifted to 537 nm when the excitation power is decreased to 1 mW/cm^2. Such a red-shift with decreasing excitation power is also present for samples A-C. For sample A this implies an emission peak shift towards the LSP resonance. As such, two competing mechanisms are present in the case of sample A when increasing the excitation power density; the first is the emission peak blue-shift, resulting in a better overlap with the LSP-mode resonance, and the second is an increase in original IQE from the increased carrier density, resulting in a reduced IQE enhancement factor from LSP-coupling. The increasing enhancement factor of sample A as seen from the inset of Fig. 6 when excitation power density is increased can therefore be expected to be the result of increasingly better spectral overlap between the QWs emission spectrum and the LSP-mode. The extinction spectra for sample B and C are relatively broad (FWHM larger than 200 nm), hence this effect would be insignificant for B and C. However, the extinction FWHM of sample A is around 50 nm, therefore an emission peak shift of about 10 nm is expected to have an effect on the LSP-QW coupling.

We also note that despite having the best spectral overlap between sample B resonance peak and the emission wavelength, sample B does not have the highest PL or IQE enhancement. This can be understood by considering the absorption and scattering properties of the Ag NPs. These effects were previously investigated and it was found that the scattering to absorption ratio is an important characteristic when determining whether Ag NPs can provide efficiency enhancement.[30] The absorption in the NP is the loss channel for the LSP mode, and reducing these losses relative to the scattering can ensure a higher LSP mode radiative efficiency. Despite the matching of the extinction or resonance peak of sample B with the emission wavelength, sample C is expected to have a higher scattering capacity at the emission wavelength due to its larger average Ag NP sizes relative to sample B.[30,33] This is because the scattering-to-absorption ratio of sample C is higher than B due to the larger Ag NPs. As such sample C is scattering dominated and sample A is absorption dominated, while sample B is in between these limits. As the emission is channeled

into the LSP mode, the scattering efficiency of the NP is crucial when energy is to be re-emitted into free-space radiation. This agrees with the parameters obtained by the fittings of Eq. (1), where sample B and C had LSP radiative efficiencies of 38 % and 45 %, respectively.

IV. CONCLUSIONS

We investigated the LSP-QW coupling and resulting IQE enhancement of GaInN/GaN QW LEDs with self-assembled Ag NPs. It was found that the strong PL enhancement was partly due to LSP-QW coupling, and partly due to LEE enhancement, and separating these effects we noted an IQE improvement due to LSP-QW coupling at 530 nm emission from 19.4% to 44.1% using large sized Ag NPs (sample C) at 756 W/cm^2. It was also found that the IQE enhancement is strongly dependent on excitation power density, yielding highest enhancement factors at low free carrier densities. Where an IQE enhancement by a factor of 2.3 was observed at 756 W/cm^2, an enhancement factor of 8.1 was observed at 1 W/cm^2. Our results confirm the inverse relation between the aforementioned quantities, and implicate that it is imperative to take the excitation power density into account when conducting PL measurements to investigate the enhancement due to LSP-coupling. We therefore establish quantitative enhancement factors depending on original IQE, and further confirm the fact that the lower the IQE of a light emitting structure is, the higher the enhancement factor will be due to surface plasmonics from Ag NPs.

ACKNOWLEDGMENTS

This work was partially supported by a Strategic Young Researcher Overseas Visits Program for Accelerating Brain Circulation from Japan Society for the Promotion of Science, the Program for the Strategic Research Foundation at Private Universities, 2012–2016, supported by the Ministry of Education, Culture, Sports, Science and Technology, and the Scandinavia-Japan Sasakawa Foundation. Y. Chen acknowledges financial support from the Danish Research Council for Technology and Production Sciences (Grant No. 10093787), and the National Natural Science Foundation of China (Grant No. 61405067). A. Fadil and H. Ou acknowledge the support of Innovation Fund Denmark (Grant No. 0603-00494B).

[1] T. Takeuchi *et al.*, "Quantum-Confined Stark Effect due to Piezoelectric Fields in GaInN Strained Quantum Wells," Jpn. J. Appl. Phys. **382**, L382, DOI:10.1143/JJAP.36.L382 (1997).
[2] C. Wetzel, T. Takeuchi, H. Amano, and I. Akasaki, "Quantized states in Ga1-xInxN/ GaN heterostructures and the model of polarized homogeneous quantum wells," Phys. Rev. B **62**, R13302-R13305, DOI:10.1103/PhysRevB.62.R13302 (2000).
[3] K. Okamoto *et al.*, "Surface-plasmon-enhanced light emitters based on InGaN quantum wells," Nat. Mater. **3**, 601–5, DOI:10.1038/nmat1198 (2004).
[4] Y. Narukawa, M. Ichikawa, D. Sanga, M. Sano, and T. Mukai, "White light emitting diodes with super-high luminous efficacy," J. Phys. D: Appl. Phys. **43**, 354002, DOI:10.1088/0022-3727/43/35/354002 (2010).
[5] E. M. Purcell, "Spontaneous emission probabilities at radio frequencies," Phys. Rev. **69**, 681 (1946).
[6] E. Yablonovitch, "Inhibited Spontaneous Emission in Solid-State Physics and Electronics," Phys. Rev. Lett. **58**, 2059-2062 (1987).
[7] S. Kühn, U. Hakanson, L. Rogobete, and V. Sandoghdar, "Enhancement of Single-Molecule Fluorescence Using a Gold Nanoparticle as an Optical Nanoantenna," Phys. Rev. Lett. **97**, 017402 (2006).
[8] D. E. Chang, A. S. Sørensen, P. R. Hemmer, and M. D. Lukin, "Quantum Optics with Surface Plasmons," Phys. Rev. Lett. **97**, 053002, DOI:10.1103/PhysRevLett.97.053002 (2006).
[9] H. Mertens, A. F. Koenderink, and A. Polman, "Plasmon-enhanced luminescence near noble-metal nanospheres: Comparison of exact theory and an improved Gersten and Nitzan model," Phys. Rev. B **76**, 115123, DOI:10.1103/PhysRevB.76.115123 (2007).
[10] A. V. Akimov *et al.*, "Generation of single optical plasmons in metallic nanowires coupled to quantum dots," Nature **450**, 402-406, DOI:10.1038/nature06230 (2007).
[11] T. Kosako, Y. Kadoya, and H. F. Hofmann, "Directional control of light by a nano-optical Yagi–Uda antenna," Nature Photonics **4**, 312-315, DOI:10.1038/nphoton.2010.34 (2010).
[12] Y. Chen, N. Gregersen, T. R. Nielsen, J. Mørk, and P. Lodahl, "Spontaneous decay of a single quantum dot coupled to a metallic slot waveguide in the presence of leaky plasmonic modes," Opt. Express **18**, 12489-12498, DOI:10.1364/OE.18.012489 (2010).
[13] Y. Chen, T. R. Nielsen, N. Gregersen, P. Lodahl, and J. Mørk, "Finite-element modeling of spontaneous emission of a quantum emitter at nanoscale proximity to plasmonic waveguide," Phys. Rev. B **81**, 125431, DOI:10.1103/PhysRevB.81.125431 (2010).

[14] Y. Nishijima, L. Rosa, and S. Juodkazis, "Surface plasmon resonances in periodic and random patterns of gold nano-disks for broadband light harvesting," Opt. Express **20**, 11466-11477, DOI:10.1364/OE.20.011466 (2012).
[15] J. Vučković, M. Lončar, and A. Scherer, "Surface plasmon enhanced light-emitting diode," IEEE Journal of Quantum Electronics **36**, 1131-1144, DOI:10.1109/3.880653 (2000).
[16] D. M. Yeh, C. F. Huang, C. Y. Chen, Y. C. Lu, and C. C. Yang, "Localized surface plasmon-induced emission enhancement of a green light-emitting diode," Nanotechnology **19**, 345201, DOI:10.1088/0957-4484/19/34/345201 (2008).
[17] C. Y. Cho *et al.*, "Surface plasmon-enhanced light-emitting diodes using silver nanoparticles embedded in p-GaN," Nanotechnology **21**, 205201, DOI:10.1088/0957-4484/21/20/205201 (2010).
[18] C. C. Kao, Y. K. Su, C. L. Lin, and J. J. Chen, "Localized Surface Plasmon-Enhanced Nitride-Based Light-Emitting Diode With Ag Nanotriangle Array by Nanosphere Lithography," IEEE Photonics Technology Letters **22**, 984-986, DOI:10.1109/LPT.2010.2049013 (2010).
[19] J. H. Sung *et al.*, "Enhancement of electroluminescence in GaN-based light-emitting diodes by metallic nanoparticles," Appl. Phys. Lett. **96**, 261105, DOI:10.1063/1.3457349 (2010).
[20] J. Henson, J. DiMaria, E. Dimakis, T. D. Moustakas, and R. Paiella, "Plasmon-enhanced light emission based on lattice resonances of silver nanocylinder arrays," Opt. Lett. **37**, 79-81, DOI:10.1364/OL.37.000079 (2012).
[21] G. Grzela *et al.*, "Nanowire antenna emission," Nano Lett. **12**, 5481–5486, DOI:10.1021/nl301907f (2012).
[22] S. R. K. Rodriguez, S. Murai, M. A. Verschuuren, and J. Gómez Rivas, "Light-Emitting Waveguide-Plasmon Polaritons," Phys. Rev. Lett. **109**, 166803, DOI:10.1103/PhysRevLett.109.16680 (2012).
[23] H. Amano, N. Sawaki, I. Akasaki, and Y. Toyoda, "Metalorganic vapor phase epitaxial growth of a high quality GaN film using an AlN buffer layer," Appl. Phys. Lett. **48**, 353, DOI:10.1063/1.96549 (1986).
[24] J. Henson *et al.*, "Plasmon enhanced light emission from InGaN quantum wells via coupling to chemically synthesized silver nanoparticles," Appl. Phys. Lett **95**, 151109, DOI:10.1063/1.3249579 (2009).
[25] C.-W. Huang *et al.*, "Fabrication of surface metal nanoparticles and their induced surface plasmon coupling with subsurface InGaN/GaN quantum wells," Nanotechnology **22**, 475201, DOI:10.1088/0957-4484/22/47/475201 (2011).
[26] S. Watanabe *et al.*, "Internal quantum efficiency of highly-efficient $In_xGa_{1-x}N$ based near ultraviolet light emitting diodes," Appl. Phys. Lett. **83**, 4906-4908, DOI:10.1063/1.1633672 (2003).
[27] K. Okamoto *et al.*, "Surface plasmon enhanced spontaneous emission rate of InGaN/GaN quantum wells probed by time-resolved photoluminescence spectroscopy," Appl. Phys. Lett. **87**, 071102, DOI:10.1063/1.2010602 (2005).
[28] Y. Lee *et al.*, "Study of the Excitation Power Dependent Internal Quantum Efficiency in InGaN / GaN LEDs Grown on Patterned Sapphire Substrate," IEEE J. Sel. Top. Quantum Electron. **15**, 1137-1143, DOI:10.1109/JSTQE.2009.2014967 (2009).
[29] G. Sun, J. B. Khurgin, and R. Soref, "Plasmonic light-emission enhancement with isolated metal nanoparticles and their coupled arrays," J. Opt. Soc. Am. B **25**, 1748-1755, DOI:10.1364/JOSAB.25.001748 (2008).
[30] A. Fadil *et al.*, "Surface plasmon coupling dynamics in InGaN/GaN quantum-well structures and radiative efficiency improvement," Sci. Rep. **4**, 1–7, DOI:10.1038/srep06392 (2014).
[31] F. D. Sala, "Free-carrier screening of polarization fields in wurtzite GaN/InGaN laser structures," Appl. Phys. Lett. **74**, 2002-2004; DOI:10.1063/1.123727 (1999).
[32] T. Kuroda and A. Tackeuchi, "Influence of free carrier screening on the luminescence energy shift and carrier lifetime of InGaN quantum wells," J. Appl. Phys. **92**, 3071-3074, DOI:10.1063/1.1502186 (2002).
[33] S. Jiang *et al.*, "Resonant absorption and scattering suppression of localized surface plasmons in Ag particles on green LED," Opt. Express **21**, 12100–12110, DOI:10.1364/OE.21.012100 (2013).